CHARACTERIZATION OF AAR IN FAGILDE DAM

Isabel Fernandes[1,*], António Santos Silva[2], José Piteira Gomes[2],
António Tavares de Castro[2], Fernando Noronha [1]

[1] Faculty of Sciences, University of Porto, Department of Geology, Rua do Campo Alegre,
4169-007 PORTO, Portugal

[2] National Laboratory of Civil Engineering, Av. do Brasil 101,
1700-066 LISBON, Portugal

Abstract

The Fagilde Dam was completed in 1984, and is located in the centre of Portugal, about 150 km SSE from Porto city. Crushed limestone was used as coarse aggregate, while alluvial siliceous sand was used as fine aggregate in the manufacture of the concrete. In the last few years, progressive displacements have been observed by the monitoring system, especially by levelling surveys. Site inspection revealed the existence of random cracking, surface discoloration, some exudation and superficial dissolution of cement in the spillways surface and in the upstream face of the dam.

In order to assess the condition of the concrete, cores were collected from various parts of the dam to perform laboratory tests. Uranyl acetate test, residual expansion tests, soluble alkalis evaluation, creep tests, unconfined compression tests and petrographic examination were carried out.

The tests performed showed the presence of different causes of deterioration that might have caused the displacements that were observed and the damage features observed.

KEYWORDS: displacement, map cracking, alkali-silica gel, expansion

1 INTRODUCTION

Fagilde Dam is a concrete structure built in the early 1980's, in the centre of Portugal, with a 26.6m maximum height over the foundation. The structure is composed of two central spillways and three buttresses, with arch sections at each side, having vertical upstream walls and artificial concrete abutments. The initial impoundment of the dam reservoir was between June 1985 and January 1987.

The monitoring system in the dam is designed for the measurement of the water level in the reservoir, atmospheric temperature, uplift water pressure, horizontal and vertical displacement by geodetical methods, joint movements and drainage flow in the foundation. In the beginning of the 1990's, irreversible displacements were registered vertical and upstream, indicating incipient deformation. Figure 1 lists the main results of the statistical model applied to the vertical displacements obtained by levelling on five points at the dam crest, between 1985 and 2006.

During the site inspection in 2001, after a second flood overflowed the dam, a set of fissures was identified, in addition to the already known map cracking in some sections of the structure. The research performed at that time concluded that alkali-aggregate reaction (AAR) was suspected as the cause of deterioration of the concrete.

In 2005, a complete research program was carried out in order to identify the causes of damage of the concrete. Core samples were extracted and examined for the presence of ASR and its extent. A number of tests were suggested which included the assessment of the mechanical characteristics of the concrete, the residual potential for alkali and/or sulfate induced expansion mechanisms, assessment of soluble alkali, and the identification of internal reactions. This study involved mechanical, chemical and petrographic tests and a multidisciplinary approach, summarized in the present paper. Work on a final report is still in progress and the modelling is not yet complete due to the long duration of some of the tests. As per today, alkali-aggregate reactions present in the concrete are considered one of the main causes of damage. However, there are other factors to consider in the final assessment of the causes of deterioration, including possible internal sulfate attack.

2 MATERIALS AND METHODS

2.1 General

A complete program of drill coring of the concrete was designed with the intent of performing a number of tests consisting of: the uranyl acetate test, residual expansion tests, soluble alkalis

* Correspondence to: ifernand@fc.up.pt

evaluation, creep tests, unconfined compression tests, and petrographic examination. Exudation samples from the surface of the cores were also collected and kept in plastic containers in order to determine the qualitative composition.

The cores were extracted by drilling equipment cooled by water. The cores were of about 150 mm in diameter for mechanical testing, and 76 mm for all other tests and analyses, with variable length, depending of the section in the structure in which they are located (Table 1).

The concrete cores were labeled with a reference number and the sample's orientation indicated with waterproof ink. To avoid desiccation, cores were wrapped in cling-film and sealed in polyethylene bags. They were immediately taken to the laboratory.

In the laboratory, the presence of alkali-silica gel was verified with uranyl acetate. After that, cores were cut with a diamond blade in order to select different portions for the various tests.

The portions for petrographic analysis were cut in half, to produce lengthwise sections. The location and orientation of thin sections were selected and signalized, namely where reaction rims, filled air voids and cracks were detected by the macroscopic analysis.

2.2 Materials and mix designs

The concrete from the Fagilde Dam is a ready-mixed concrete of the class of resistance C16/20 [1] with a CEM I type cement content of 360 $kg \cdot m^{-3}$. Aggregates are of two types: a coarse aggregate fraction composed of crushed limestone from a quarry, and a fine fraction (sand) of siliceous composition, from an alluvial deposit. It was not possible to identify the exact provenance area of the aggregates.

2.3 Methods for assessment and analysis

Mechanical tests

Mechanical tests were carried out during the 2005 program, on core samples measuring 150 mm diameter (core numbers 2, 4, 6 and 9). Unconfined compression and diametrical compression tests were performed compliant with Portuguese standard E 226 [2] on cylindrical samples of 150mm height. Concrete cylinders with 600 mm height were used in the elasticity modulus determination, performed according to the Portuguese standard E 397 [3].

Residual alkali-silica reactivity of concrete

Concrete cores 76 mm diameter and 160 mm in length were tested according the LPC nº 44 test method [4]. Of the 72 specimens tested, 26 were tested with external supply of alkalis (Table 1). In this method the specimens, previously wrapped in absorbent paper and polyethylene sheet, are placed in a closed metal container, with a few centimetres of water or 1M NaOH solution, and placed in a climatic chamber at 38ºC. The measurements are made at various intervals over the period of one year, with a gauge length comparator (0.001 mm resolution) adapted to the shape of the reference studs installed at the ends of each core. Some cores were crushed one year after extraction for assessment by scanning electron microscope (SEM) JEOL JSM-6400, coupled with an OXFORD energy dispersive spectrometer X-ray detector (EDX). The samples were sputtered with carbon in a JEOL JEE-4X vacuum evaporator to avoid charging.

Residual internal sulfate reactivity of concrete

Concrete cores, with the same dimensions of those previously mentioned, were tested according the LPC nº 66 test method [5,6]. In this method, the expansion is obtained by lateral length measurements in three equally spaced lines of two gauge reference studs each, with a distance of 100 mm between the two studs of a given line, thus permitting three readings per core. The specimens are immersed in tap water at 20±2ºC. The measurements were made at regular intervals with a gauge length comparator adapted to the reference studs installed in the three laterals lines of each core. As in the ASR residual reactivity, one year after immersion, some of the cores were analysed by the SEM/EDX equipment.

Content soluble alkali

About 250 g of concrete was crushed and reduced to pass 160 μm and oven dried at 40ºC for one day and was reduced by manual splitting to ~50 g sufficient samples to fill a porcelain vibratory ball-mill for pulverization. Alkali determination was conducted following the methodology developed by Bérubé et al. [7], with sodium and potassium contents determined separately on a GBC 906AA atomic absorption spectrometer (AAS).

Petrographic microscope observations

Petrographic analysis of the concrete included macroscopic assessment of the concrete cores as extracted, prior to thin section or other preparation.

During storage, white exudations were formed in the surfaces of the cores. Samples of these exudations were glued with araldite to metallic cylinders 6 mm diameter, submitted to vacuum and sputtered with gold in a JEOL JFC 1100 instrument.

Slices of the concrete were cut and glued with araldite to a glass slide to produce thin sections measuring 25×45 mm. The samples were impregnated with resin to avoid permeability and loss of material by heating at T <70º C until dried, without application of vacuum. Thin sections of 30 μm thickness were produced by hand using several stages of grinding and lapping with powdered silicon carbide until final polishing with 0.25 μm diamond grit. The thin sections were polished for examination by SEM and determination of qualitative analysis by EDX.

Thin sections were observed in a Nikon Eclipse E400POL petrographic microscope in plane polarized light (PPL) and crossed polarized light (XPL). Locations of alkali-silica gel were identified with ink on the thin section surface. They were then sputter-coated with carbon under vacuum in a VG MICROTECH E6700/T800 instrument for analysis by scanning electron microscope JEOL JSM-6301F equipped with field-emission gun (FEG), and a NORAN-VOYAGER energy dispersive spectrometer (EDX). Acceleration voltage was set to 15kV, beam current to 10nA, and working distance of 15 mm. The collection time for the microanalyses was 60 seconds with a dead time of approximately 30%. Spot size was set to 10nm for qualitative analysis.

3 RESULTS

3.1. Site inspection

The inspection of the concrete surfaces showed that there is cracking and discoloration in some sections of the structure, more prominent in the downstream faces of the lateral arches and in the spillway surfaces (Figure 2). In the upstream face and in the surface of the spillways there is a set of horizontal fissures and also intense map cracking. The concrete surface is not smooth and shows features of dissolution both of the cement paste and of some of the particles of aggregate. There are siliceous grains of the fine aggregate that are exposed and protruding from the surrounding paste. The buttresses also have map cracking which is particularly intense in the northern faces. Rare exudations composed of calcium carbonate were found, some associated with the horizontal cracks.

3.2. Macroscopic analysis of concrete cores

The concrete cores were visually in a sound state and showed homogeneous distribution of the aggregate particles throughout the material. Some cores show a higher porosity and in others there are voids with irregular shapes occurring among close particles of coarse aggregate, where cement paste seems not to have penetrated. When drying, damp patches could be observed close to some of the particles of aggregate (Figure 3), mainly in the cores showing higher porosity. There are also light coloured rims on the aggregate boundaries and rare, brownish rims in the cement paste around the particles of coarse aggregate.

Rare fine cracks were identified in the cement paste and partially around the boundaries of some coarse aggregate particles. Some voids show a white lining.

Aggregates are mainly composed by angular particles, some elongated, of a carbonate rock and also some siliceous rock fragments. The D_{max} of coarse aggregates is of 3 to 5 mm, as measured in the halved cores. The uranyl acetate test was performed in the complete length of the cores. However, the results were not conclusive as just a few greenish spots were observed under UV light.

3.3. Mechanical tests

In order to evaluate the present characteristics of the concrete, mechanical tests were performed on samples from the arch sections and from the buttresses of the dam.

The results from unconfined compression show a high compressive strength of the concrete. The average value is of 33.7 MPa and the minimum is 21.1 MPa, when referenced to cubes measuring 200 mm on a side. These values are, according to [1], characteristic of a C20/25 class of concrete, which is higher than that defined in the design of the structure. Considering that the initial compressive strength of the concrete should correspond to the values defined in NP EN 206 [1], it can be concluded that the deterioration process could not have affected significantly the compressive strength of the concrete.

Concerning the diametrical strength, an average of 3.0 MPa was obtained and a minimum of 2.25 MPa, which indicates that, for a class C20/25, the tensile strength is a little lower than expected.

The elasticity modulus was obtained on four samples and presents values between 19.1 GPa, in the left buttress, and 24.4 GPa. A value of 31.4 GPa was obtained in a specimen with 500 mm height.

3.4. Residual alkali-silica reactivity and internal sulfate

Tests for assessing the potential for further ASR expansion started in December 2005. The results obtained with these tests are presented in Table 2. It was verified that specimens exposed to water moisture experienced higher values of residual expansion than those stored in the alkali solution.

The specimens were observed by SEM after the completion of the tests. The SEM revealed the presence of ettringite in all specimens, occurring in a compressed form in the paste-aggregate interfaces, which was attributed to an internal sulfate reaction (Figure 4). Besides the presence of ettringite, some ASR products were detected, with characteristic shrinkage cracks and a smooth surface. Determination of residual internal sulfate reactivity of the Fagilde concrete was commeced in 2007, results are not available at present.

3.5. Content of soluble alkalis in water

In order to determine if the alkalis content would be sufficient to maintain the ASR and to evaluate possible variations on soluble alkalis in the structure, specimens were selected close to the sites where samples for residual expansion were taken. It was verified that the higher alkali soluble contents were obtained in core number 11, which was located a greater distance from the upstream wall, where damage is more intense.

Assuming a concrete density of 2400 $kg \cdot m^{-3}$, values of 1.73 and 3.00 kg of Na_2O_{eq}/m^3 are calculated for the concrete in the arch sections, with a greater range of values in the left section (Figure 5). The buttresses contain calculated values between 1.62 and 4.28 kg of Na_2O_{eq}/m^3.

3.6. Petrographic microscope observations

The petrographic analysis was conducted with two objectives: (1) evaluation of the potential reactivity of aggregates to alkalis and (2) the detection of possible microscopic manifestations of deterioration in the concrete.

Potential reactivity of aggregates

The composition and nature of the aggregates were identified by the examination of thin sections. The coarse aggregates are composed dominantly by micritic (carbonated mudstone) limestone containing veinlets of sparitic (crystalline) calcite. In some grains there are individualized crystals with interstices filled by brownish minerals. The observation of these particles by SEM/EDX permitted the detection of finely dispersed microsilica and silicates that might correspond to mica or clay minerals. In the limestone rock, remains of fossils were identified filled by a mineral of radial texture and low birefringence. It was concluded by SEM/EDX that the fossils are filled by chalcedony and calcium carbonate and alkali-silica gel is also present (Figure 6).

The coarse fraction also includes well rounded siliceous particles composed of various forms of polycrystalline quartz. Some grains show microcrystalline quartz, classified as potentially reactive according to the RILEM AAR-1 [8] report and also by the Portuguese standard E LNEC 461 [9].

The sand fraction particles are dominantly well rounded, rich in monocrystalline and polycrystalline quartz, including microcrystalline textures, silicate minerals, such as K-feldspar, plagioclase, biotite, chlorite, muscovite, epidote, tourmaline and opaque minerals. There are also fragments of rocks such as granite, limestone and schist.

Manifestations of internal reactions

The most prominent characteristic of the concrete in Fagilde Dam is the presence of microcracking in the interfaces between coarse aggregate particles and the cement paste. These cracks reach 120 μm in width, are discontinuous around the particles and some extent into the cement matrix. Most are filled by crystals of ettringite growing perpendicular to the walls. Ettringite crystals are also present in voids and in the cement paste.

In some places the coarse aggregate particles of limestone show diffuse boundaries (Figure 7) or carbonate halos. These grains contain microsilica and silicates in the interstices, as above referenced. Element maps produced show the presence of calcium in different concentration, as well as silicon and aluminium. The contents of sodium, potassium and magnesium are very low.

There are cracks passing through the cement paste and through some of the siliceous aggregate particles. The presence of ASR gel is heterogeneous along the structure and also in each concrete core.

The gel is present in some cracks but dominantly substitutes siliceous particles of the sand fraction. It is a colourless gel in the rims of the particles and voids, isotropic, with typical shrinkage cracks. In the interior of the substituted particles, the gel is brownish. SEM/EDX observation showed that the gel is composed mainly of silicon, calcium, potassium, and some aluminium, sodium and magnesium (Figure 8).

It was verified that the cement paste appears lighter in colour close to the coarse aggregate grains and to the cracks, suggesting a higher porosity. The interface with the darker paste is irregular. In some thin sections, taken from sites near or at the exposed walls of the concrete, carbonation of the cement paste is visible. The exudations formed in the surface of the cores are also composed of alkali-silica gel, as confirmed by SEM/EDX.

4 DISCUSSION

The site inspection and the visual observation of the concrete cores revealed the existence of features related to the occurrence of ASR. The damp patches and brownish rims around some of the aggregate particles are consistent with this conclusion.

The uranyl acetate test was not conclusive, as results seemed to be influenced by other factors besides possible ASR.

The mechanical tests demonstrated that the unconfined compression strength is not affected by the deterioration of the concrete but that the tensile strength and the elasticity modulus are lower than expected, as referenced in literature [10, 11]. This fact might be attributed to the microcracking, in particular the cracks partially around the aggregate boundaries. These cracks are probably the result of poor bonding, debonding between the two components or poor workmanship during the mixing and placing of the concrete.

The residual alkali-silica expansion tests indicate that the specimens in water vapour experienced higher values than those with added alkalis, which can be explained by a depletion of the sources of reactive silica in concrete. The images obtained by SEM/EDX confirm the formation of either alkali-silica gel and ettringite crystals.

Concerning the content of soluble alkalis test, it was verified that the values are relatively high. According to literature [eg. 10], a content of 3.6 $kg \cdot m^{-3}$ would be the maximum permissible to prevent deleterious ASR in concrete. It was confirmed that values exceeding that limit were obtained for the buttresses, in particular in core 11, meaning there are still alkalis available for reaction.

The petrographic analyses confirmed the presence of alkali-silica gel replacing siliceous particles, in voids and in some cracks. The characteristics of this gel and its qualitative composition are consistent with other results published [12,13,14] being rich in silicon with calcium, potassium and sodium. The alkali-silica gel in not homogeneously distributed through the structure and also shows an irregular presence along a single core. It seems to be concentrated in specific places and in cores that exhibit higher porosity.

In the thin sections it was observed that the most widely distributed product of internal reaction is ettringite, which occurs with a more homogeneous distribution in the structure, when compared to the alkali-silica gel. Cracks exist around the coarse aggregate particles and also around some of the grains of the sand fraction. They extend into the cement paste and are filled with ettringite crystals growing perpendicular and parallel to the walls of the cracks.

The diffuse limits between the limestone grains and the cement paste and also the brownish rims around some aggregate grains suggest the occurrence of alkali-carbonate reactions as suggested by Katayama [15]. However, the element maps made did not reveal the presence of significant Mg well above the detection limit (~0.1-10wt%). The intergranular porosity provides a pathway for easy access of alkali and fluids to the microcrystalline silica in the limestone. The presence of exudations surfaces on the core surfaces provides evidence that ASR is developing in the concrete.

5 CONCLUSIONS

A wide range of tests was performed on the concrete of Fagilde Dam to evaluate the cause and the extent of damage in the structure. According to above results, the phenomena observed in the dam concrete as well as its displacements, can be summarized as follows:

- Irreversible upward vertical displacements have been measured at the dam crest, indicative of a concrete expansion process;
- Cracks and manifestations of dissolution of the surface concrete were identified on site;
- Mechanical tests show that unconfined compressive strength has not been affected by the deterioration of the concrete, but that damage did affect elasticity modulus of the concrete;
- Cracks are frequent in the interface of coarse aggregate particles-cement paste;

- Alkali-silica gel is present in voids and mainly in substitution of siliceous aggregate particles;
- Exudations in the core surfaces are composed of alkali-silica gel, showing that the alkali-silica reaction is developing;
- Ettringite is widely distributed in the concrete and is abundant in voids, cracks in the boundaries of aggregate particles, and in the cement paste;
- Internal sulfate attack is probably the main cause of deterioration, associated with the formation of alkali-silica gel in some sections of the dam.

6 ACKNOWLEDGMENTS

The present work was developed in the scope of the research project GRANMAT - POCTI/CTA/45936/ 2002 financed by FCT - Fundação para a Ciência e a Tecnologia.

7 REFERENCES

[1] NP EN 206 (2005): Betão. Parte 1: Especificação, desempenho, produção e conformidade. IPQ, Lisbon: pp 84.
[2] E 226 (1968): Betão - Ensaio de compressão. LNEC, Lisbon: pp2.
[3] E 397 (1993): Betões – Determinação do módulo de elasticidade. LNEC, Lisbon : pp2.
[4] LPC 44 (1997): Alcali-réaction du béton. Essai d'expansion résiduelle sur béton durci. LCPC, Paris: pp 12.
[5] LPC 66 (2007): Réactivité d'un béton vis-à-vis d'une réaction sulfatique interne – Essai de performance. LCPC, Paris: pp 17.
[6] Pavoine, A, Divet, L and Fenouillet, S (2006): A concrete performance test for delayed ettringite formation: Part 1 optimization, Cement and Concrete Research (36): 2138-2143.
[7] Bérubé, MA, Frenette, J, Rivest, M and Vézina, D (2000): Measurement of the alkali content of concrete using hot-water extraction. In: Bérubé, MA, Fournier, B, and Durand, B (editors): Proceedings of the 11th International Conference on Alkali-Aggregate Reaction in Concrete, Québec, QC, Canada: 159-168.
[8] Sims, I, and Nixon, P (2003): RILEM Recommended Test Method AAR-1 (2003): Detection of potential alkali-reactivity of aggregates – Petrographic method, TC 191-ARP: Alkali-reactivity and prevention. Assessment, specification and diagnosis of alkali-reactivity. Materials and Structures (36): 472-479.
[9] Especificação LNEC E461 (2004): Betões. Metodologias para prevenir reacções expansivas internas. LNEC, Lisbon: pp 6.
[10] Hobbs, DW (1988): Alkali-silica reaction in concrete. Thomas Telford Ltd. London: pp183.
[11] Ben Haha, M (2006): Mechanical effects of alkali silica reaction in concrete studied by SEM-image analysis. PhD Thesis, École Polytechnique Fédérale de Lausanne, Switzerland: pp176.
[12] Thaulow, N, Jakobsen, UH, and Clark, B (1996): Composition of alkali silica gel and ettringite in concrete railroad ties: SEM-EDX and X-ray diffraction analyses. Cement and Concrete Research (26): 309-318.
[13] Fernandes, I, Noronha, F, and Teles, M (2004): Microscopic analysis of alkali-aggregate reaction products in a 50-year-old concrete. Materials Characterization (53/2-4), Special Issue (29): 295-306.
[14] Shayan, A, and Grimstad, J (2005): Deterioration of concrete in a hydroelectric concrete gravity dam and its characterization. Cement and Concrete Research (36): 371-383.
[15] Katayama, T (2004): How to identify carbonate rock reactions in concrete. Materials Characterization (53/2-4), Special Issue (29): 85-104.

TABLE 1: Drill cores obtained for the study of deterioration of the concrete of Fagilde Dam and the number of tests performed in each drill core.

Drill core reference	*Length (m)*	*Petrographic analyses*	*Unconfined compression tests*	*Soluble alkali content*	*ASR residual expansion*		*Residual internal sulfate*
					Water	*NaOH 1N*	
1	9,60	3	-	3	6	3	-
2	5,00	-	1	-	-	-	-
3	14,15	4	-	4	7	4	1
4	5,00	-	1	-	-	-	-
5	27,30	6	-	6	8	4	2
6	5,00	-	1	-	-	-	-
7	27,00	7	-	6	10	6	2
8	14,15	4	-	4	5	3	2
9	5,00	-	1	-	-	-	-
10	8,2	3	-	3	4	2	2
11	20,95	5	-	5	6	4	2

TABLE 2: Residual expansion of specimens immerged in water.

Location		*Residual expansion (x10^{-6})*	
Structure section	*Core*	*Max.*	*Min.*
Right arch	1	900	350
	3	440	150
Right butress	5	350	120
	11	600	220
Left arch	8	480	260
	10	600	280
Left butress	7	580	300

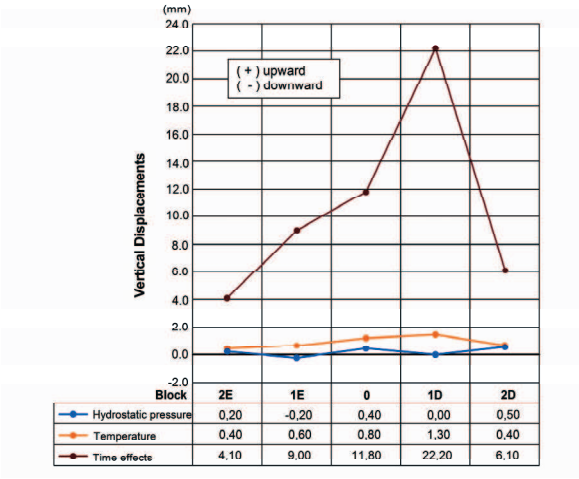

Figure 1: Main results of statistical model of the vertical displacements observed between 1985 and 2006.

Figure 2: Horizontal cracks and map cracking in the right buttress and in the right arch.

Figure 3: Concrete cores showing different characteristics in the macroscopic analysis. In the core at the left hand side voids are present close to coarse aggregate particles; the core in the centre shows damp patches around aggregate particles and higher porosity; the right hand side exhibits an exudation of alkali-silica gel (core diameter: 76 mm).

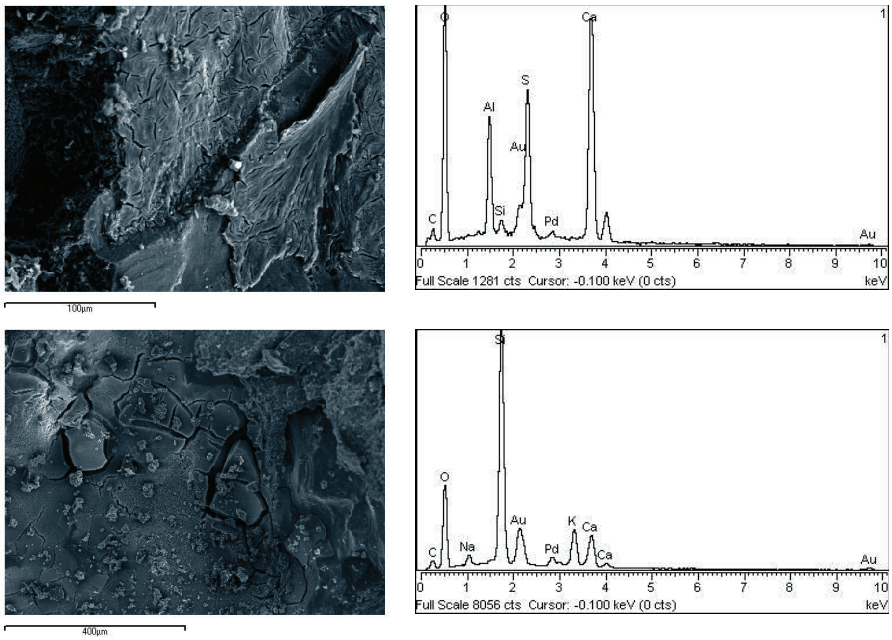

Figure 4: Samples observed by SEM after the residual alkali-silica reactivity tests. Spectra obtained by EDX confirm the presence of ettringite and alkali-silica gel.

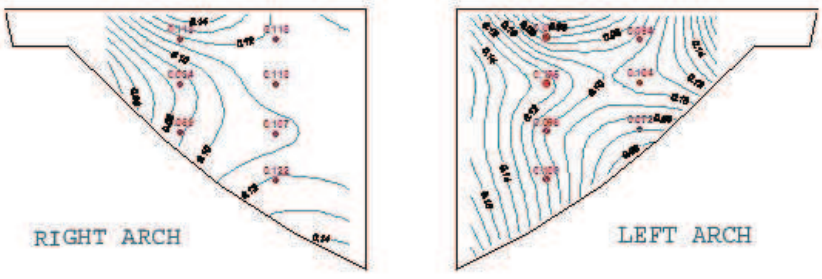

Figure 5: Distribution of soluble alkalis in percentage of bulk concrete on the right and left arch sections.

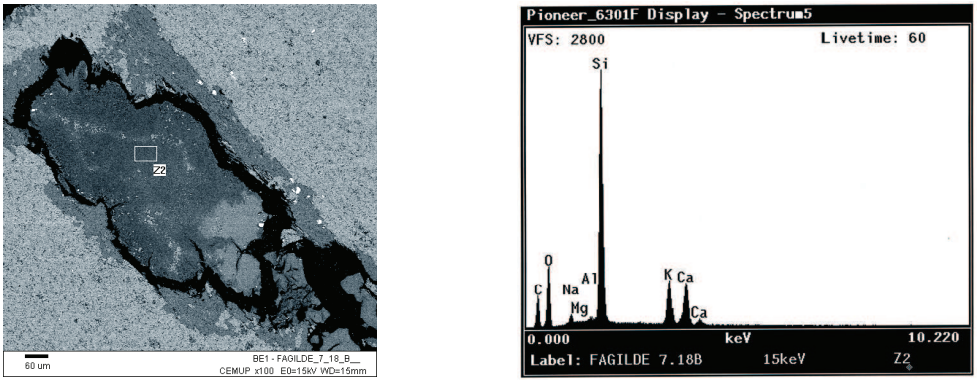

Figure 6: Fossil remains included in a particle of micritic limestone are composed of chalcedony. The EDX analysis shows the presence of alkali-silica gel (image in XPL, SEM and spectrum by EDX) (SEM image and spectrum obtained by CEMUP).

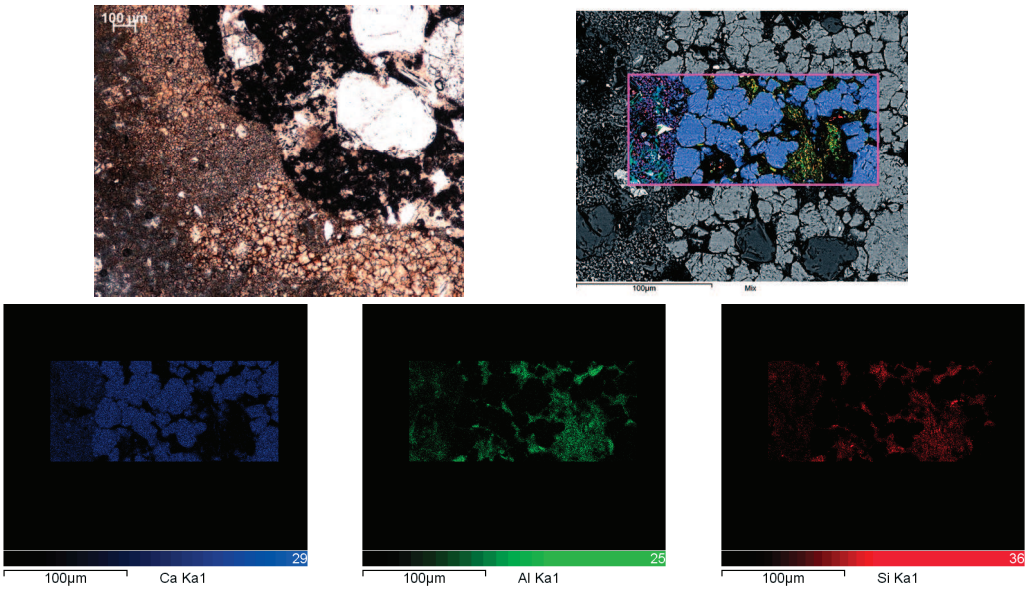

Figure 7: Interfaces between coarse aggregate particles and the cement paste are in some places diffuse (images in PPL and by SEM). Maps of elements obtained by EDX (SEM image and spectra obtained by CEMUP).

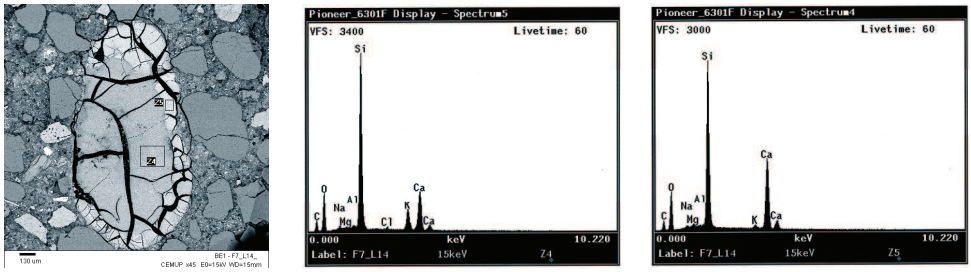

Figure 8: Alkali-silica gel replacing completely a quartz particle (SEM/EDX) (image and spectra obtained by CEMUP).